Chapter 14. SURFACE IMPOUNDMENT ELEMENT MODEL DESCRIPTION

M.R. Lindley, B.J. Barfield and B.N. Wilson

14.1 Introduction

User requirements dictate that the WEPP Surface Impoundment Element (WEPPSIE) must simulate several types of impoundments: farm ponds, terraces, culverts, filter fences, and check dams (Foster and Lane, 1987). In order to determine the impact of sediment-laden runoff, the user needs to know:

1. Peak outflow rate and outflow volume.
2. Peak effluent sediment concentration and total sediment yield.
3. Time to fill an impoundment with sediment.

To meet these requirements, the WEPPSIE code includes five sections: a front-end interface, daily input, hydraulic simulation, sedimentation simulation, and daily output. A flow chart illustrating how the WEPPSIE code is integrated into the overall WEPP model is shown in Fig. 14.1.1.

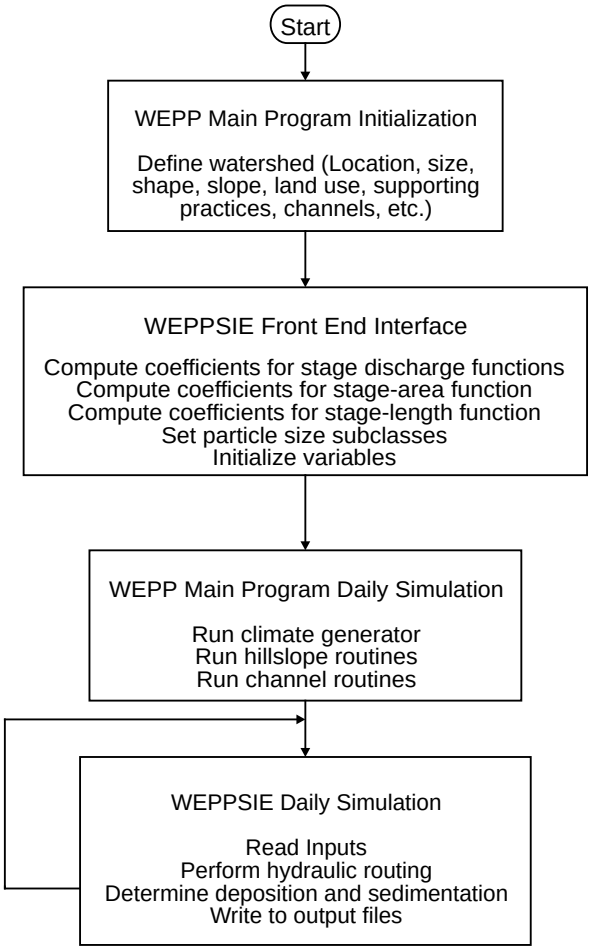

Figure 14.1.1. Flow chart for WEPPSIE.

The front-end interface is run only once at the beginning of a WEPP simulation. Within the front-end interface, the coefficients of continuous stage-discharge relationships are determined from information entered by the user, describing each outflow structure present in a given impoundment. The user can enter information on one or more of the following possible structures:

1. Drop spillway.
2. Perforated riser.
3. Two sets of identical culverts.
4. Emergency spillway or open channel.
5. Rock-fill check dam.
6. Filter fence or a straw bale check dam.

The user also has the option of entering a discrete stage-discharge relationship. For structures that are too hydraulically complex to allow for a direct solution of outflow for a given stage, the coefficients for continuous, directly solvable equations are developed using nonlinear regression. The coefficients for continuous stage-area and stage-length equations are also developed in the front-end interface. The input section of WEPPSIE receives daily hydraulic inputs and sedimentologic inputs from the hillslope and channel components. Hydraulic inputs as defined by the WEPP convention consist of incoming storm volume and incoming flow rate using a rectangular hydrograph shape. Sediment inputs include total suspended sediment concentration in each particle size class (clays, silts, sands, small aggregates, and large aggregates). The size class divisions are based upon the CREAMS criteria (Foster et al., 1985; USDA, 1980) and the median particle size diameter.

The hydraulic simulation section of the impoundment element performs a direct numerical integration of an expression of continuity. An adaptive time step is utilized which increases the time step when the inflow and outflow rates are relatively constant. A temporary file of the predicted outflow hydrograph including the time, stage and outflow at each time step included in the integration is created.

The sedimentation simulation section determines the amount of sediment deposited and the outflow concentration for each time step. Deposition and effluent sediment concentration are predicted using conservation of mass and overflow rate concepts. Two calibration coefficients are included in the deposition procedures to account for impoundment geometry, hydraulic response, and stratification.

The output section creates output files for the user. Output files provide the user with daily information and yearly summaries. Information output to the user includes:

1. Peak inflow rate and inflow volume.
2. Peak outflow rate and outflow volume.
3. Peak stage and overtopping times.
4. Peak influent sediment concentration and influent sediment mass.
5. Peak effluent sediment concentration and total sediment discharge.
6. Break down of influent and effluent sediment mass by particle size class.
7. Time to fill an impoundment with sediment.

In this model development chapter, the hydraulic routing procedure is first discussed. Then the stage-discharge and stage-area relationships developed in the front-end interface are described in detail. Finally, the procedures used in determining the amount of sediment deposited in the impoundment and the amount of sediment leaving the impoundment are described.

The user of the model should be alerted to potential problems with dimensions on model variables. The variables used in the calculations in the model are given in the list of variables at the end of this chapter. However, the input parameters do not have the same dimensions as those used in this chapter. Conversions are made in an interface between the remainder of the WEPP model and the impoundment element. For example, the length variables in this chapter are typically feet whereas the input parameters in WEPP are typically meters. In the interface, the appropriate conversions are made.

Exceptions to the use of SI units in the WEPP model inputs will be found. In some cases, parameter values are not readily available in metric units. For example, head loss relationships for culverts are readily available in English units, but not in metric. In those cases, the inputs are in English units.

It is important that the user refer to the most recent version of the User Summary document to determine the appropriate units for WEPP model inputs.

14.2 Hydraulic Routing

The WEPP Surface Impoundment Element must function on the five types of impoundments described earlier. Since WEPP is a continuous simulation model that runs on a daily basis, the impoundment element must also run as a continuous simulation model, updated on a daily basis. To determine the hydraulic routing for each day, the impoundment element utilizes the principle of continuity including functional stage-area and stage-discharge relationships. The hydraulic inputs and outputs for the impoundment element are defined by the WEPP convention as rectangular hydrographs formed by the peak inflow or outflow rate and the incoming or exiting volume for each twenty-four hour period.

14.2.1 Continuity Expression

The basis for hydraulic routing is the traditional expression of continuity (Haan et al., 1994):

$$\frac{dV}{dt} = Q_i - Q_O \qquad [14.2.1]$$

where V is impoundment volume (ft^3), t is time (s), Q_i is the inflow rate ($ft^3 \cdot s^{-1}$), and Q_o is outflow rate ($ft^3 \cdot s^{-1}$). If the volume is split into stage and area, and both sides of the continuity expression are divided by area, the expression becomes:

$$\frac{dH}{dt} = \frac{Q_i - Q_o}{A_{imp}} \qquad [14.2.2]$$

where H is stage (ft) and A_{imp} is impoundment area (ft^2). Since WEPP utilizes a rectangular inflow hydrograph, the inflow in Eq. [14.2.2] is constant. Thus, for any twenty-four hour period simulated, the inflow is at the constant peak inflow until the inflow volume has entered the impoundment, after which the inflow is zero.

The outflow, Q_o, in Eq. [14.2.2] depends upon the type of outlet structure, and its dimensions. Given the type and size of the outlet structure, the outflow, Q_o, is functionally related to the difference between water surface stage and the inlet stage of the outlet structure, called the driving head, or:

$$Q_o = f_{Q_o}(H) \qquad [14.2.3]$$

The functional relationship is also dependent upon the water surface stage. In some impoundments, more than one outlet structure is utilized, as in the case of a traditional farm pond with a drop-inlet spillway and an emergency spillway. In this case, the functional relationship in Eq. [14.2.3] takes one form when there is flow only through the drop-inlet spillway, and another form when there is also flow through the emergency spillway. In this chapter, an outflow regime is defined as the range of water surface stages in which the functional relationship in Eq. [14.2.3] takes on a certain form. When the functional relationship in Eq. [14.2.3] changes form, as in the case when flow changes from flowing only

through a drop-inlet spillway to flowing through both a drop-inlet spillway and an emergency spillway, the flow is said to have transitioned from one outflow regime to another. A detailed discussion on how the outflow, Q_o, is determined for all of the possible outlet structures is presented in the Stage-Discharge Relationships section of this chapter.

The area, A_{imp}, in Eq. [14.2.2] is also related to the stage of the water surface, depending upon the topography of the impoundment, or:

$$A_{imp} = f_A(H) \qquad [14.2.4]$$

A detailed discussion on how the functional relationship between area and stage is developed is presented in the Stage-Area Relationship section of this chapter.

Inserting Eq. [14.2.3] and [14.2.4] into Eq. [14.2.2] yields:

$$\frac{dH}{dt} = \frac{Q_i - f_{Q_o}(H)}{f_A(H)} \qquad [14.2.5]$$

The continuity expression given in Eq. [14.2.5] shows that the change in stage over time is entirely related to the inflow rate and two functional relationships to stage. The hydraulic routing procedure utilized by WEPPSIE involves the performance of a direct numerical integration of the continuity expression. To get a new stage point, given the current stage point, Eq. [14.2.5] must be integrated over time with the proper stage-discharge relationship. From the new stage, the new outflow can be determined with the stage-discharge relationship. As the numerical integration proceeds over time, the outflow hydrograph is formed.

The outflow hydrograph required by WEPP is formed solely by the peak outflow and the total outflow volume for a simulated twenty-four hour day. Equation [14.2.5] can be converted to a variable inflow by either using the breakpoint inflow or parameterizing the inflow hydrograph.

14.2.2 Runge-Kutta Numerical Integration

To integrate the continuity expression given in Eq. [14.2.5], a classical fourth-order Runge-Kutta numerical integration is employed which has been adapted from Press et al. (1986). For a given time step, the new head, H_{new} (*ft*), is calculated from four separate estimates of *dH/dt*, the differential change in stage with respect to time given in Eq. [14.2.5]. First, *dH/dt* is evaluated at the current time and stage, at two trial midpoints, and then at a trial endpoint. This approach gives an error term on the order of Δt^5. The procedure is organized as follows to compute a new stage, H_{new}, from the current stage, H (*ft*), the current time, t (*s*), and a time step, Δt (*s*):

$$
\begin{aligned}
\Delta H_1 &= \Delta t \left[\frac{dH}{dt}\right]_{(t,\ H)} \\
\Delta H_2 &= \Delta t \left[\frac{dH}{dt}\right]_{\left(t+\frac{\Delta t}{2},\ H+\frac{\Delta H_1}{2}\right)} \\
\Delta H_3 &= \Delta t \left[\frac{dH}{dt}\right]_{\left(t+\frac{\Delta t}{2},\ H+\frac{\Delta H_2}{2}\right)} \\
\Delta H_4 &= \Delta t \left[\frac{dH}{dt}\right]_{\left(t+\Delta t,\ H+\Delta H_3\right)} \\
H_{new} &= H + \frac{\Delta H_1}{6} + \frac{\Delta H_2}{3} + \frac{\Delta H_3}{3} + \frac{\Delta H_4}{6} + O(\Delta t^5)
\end{aligned}
\qquad [14.2.6]
$$

Figure 14.2.1 from Press et al. (1986) graphically illustrates the locations for which *dH/dt* is evaluated in the procedure.

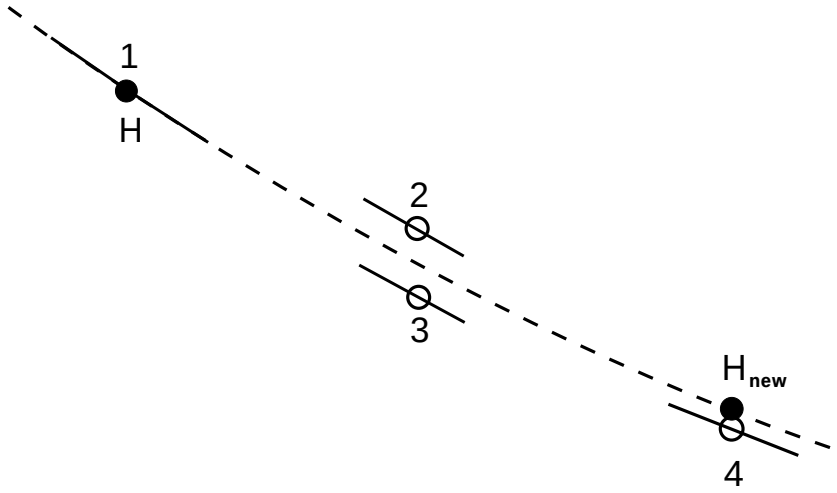

Figure 14.2.1. Illustration of Runge-Kutta integration (Press et al., 1986).

14.2.3 Adaptive Time Step

All computations begin at an initial time step referred to as the minimum time step. At the beginning and end of inflow, and when flow transitions from one outflow regime to another, the time step is set to the initial "minimum value." To increase the speed of the Runge-Kutta numerical integration procedure, an adaptive step size has also been incorporated from Press et al. (1986). This adaptive step size procedure increases or decreases the time step, Δt, until the error in the prediction of H_{new} is just below a maximum acceptable error. First, the new stage is computed by taking two successive time steps of $\Delta t/2$ then the new stage is computed by taking one time step of Δt. The difference between these two new stages is called the *error*. If the *error* is less than the specified maximum error, $E_{\max}$ (*ft*), then the next time step is increased. If the *error* is less than a minimum error, $E_{\min}$ (*ft*), then the next time step is

four times greater than the current time step:

$$\Delta t_{next} = 4\Delta t \qquad [14.2.7]$$

If the *error* is between $E_{\min}$ and $E_{\max}$ then the next time step is increased relative to the current time step by (Press et al. 1986):

$$\Delta t_{next} = 0.9\Delta t \left(\frac{error}{E_{\max}} \right)^{-0.2} \qquad [14.2.8]$$

If the *error* is greater than $E_{\max}$ then the current time step is decreased to (Press et al., 1986):

$$\Delta t_{next} = 0.9\Delta t \left(\frac{error}{E_{\max}} \right)^{-0.25} \qquad [14.2.9]$$

and the computation of the new stage is attempted again from the beginning. (Note: the exponents -0.20 and -0.25 in Eq. [14.2.8] and [14.2.9] are correct.) Currently, $E_{\max}$ is 10^{-4} feet and $E_{\min}$ is 6 x 10^{-7} feet.

The new stage is also checked to be sure that it is within the same outflow regime. If the new stage indicates that the outflow regime has changed, the time step is decreased to an initial minimum time step and attempted again. At the beginning and end of inflow, the time step is also set equal to the initial minimum time step. Thus, at each point where the outflow function used in Eq. [14.2.5] changes, the time step is set equal to the initial minimum time step. The adaptive step size begins to increase or decrease the time step from this initial minimum time step to develop the desired accuracy. Currently the minimum time step utilized ranges from 0.01 to 0.1 hr, at the user's discretion.

14.3 Stage-Discharge Relationships

Stage-discharge relationships are developed from information the user enters about each outflow structure incorporated into a given impoundment. To save computation time, the front-end interface is utilized to develop coefficients for explicit continuous outflow functions for each possible outflow structure. This is done once at the beginning of a WEPP run. For structures such as: drop spillways, culverts, rock-fill check dams, filter fence, and straw bale check dams, explicit stage-discharge functions can be developed directly from the dimensions of the outflow structure entered by the user. For structures with more complex stage-discharge relationships that require iterative solutions for the discharge for a given stage, regression equations are utilized as explicit stage-discharge functions.

WEPPSIE can function with any combination of the following outlet structures:

1. Drop spillway.
2. Perforated riser.
3. Two sets of identical culverts.
4. Emergency spillway or open channel.
5. Rock-fill check dam.
6. Filter fence or a straw bale check dam.

or the user can enter a discrete stage-discharge relationship. Thus, the outflow function, $f_{Qo}(h)$, used in the continuity expression, Eq. [14.2.5], must be defined for the entire range of possible water surface stages for any combination of possible outlet structures. In order to cover all the possibilities, $f_{Qo}(h)$, is a summation of the outflow contributions from each possible outlet structure. If a structure is not present, or if the water surface stage is below the inlet of the structure, then the contribution of that outlet structure

to the total outflow is zero. If there is flow through one or more outlet structures, the flows are summed to yield the total outflow.

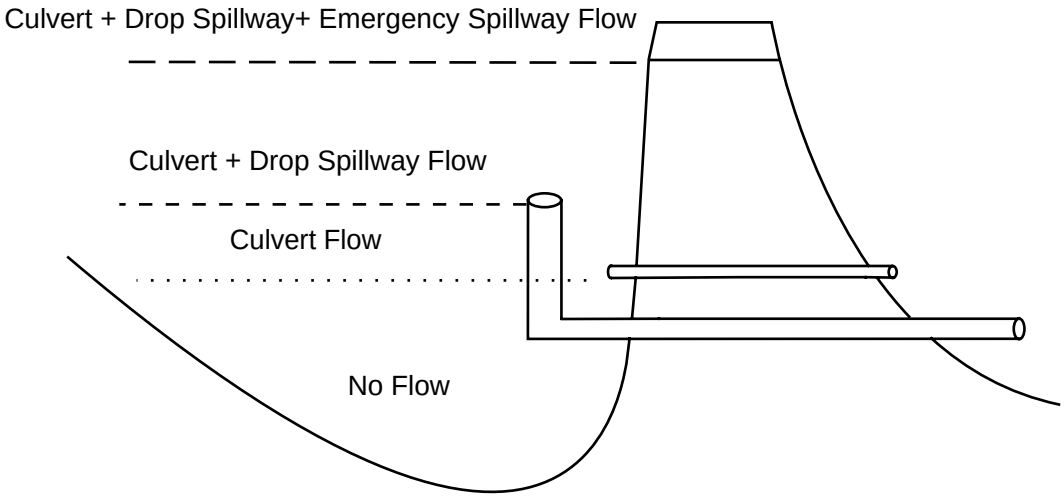

Figure 14.3.1. Schematic of an impoundment with multiple outlet structures.

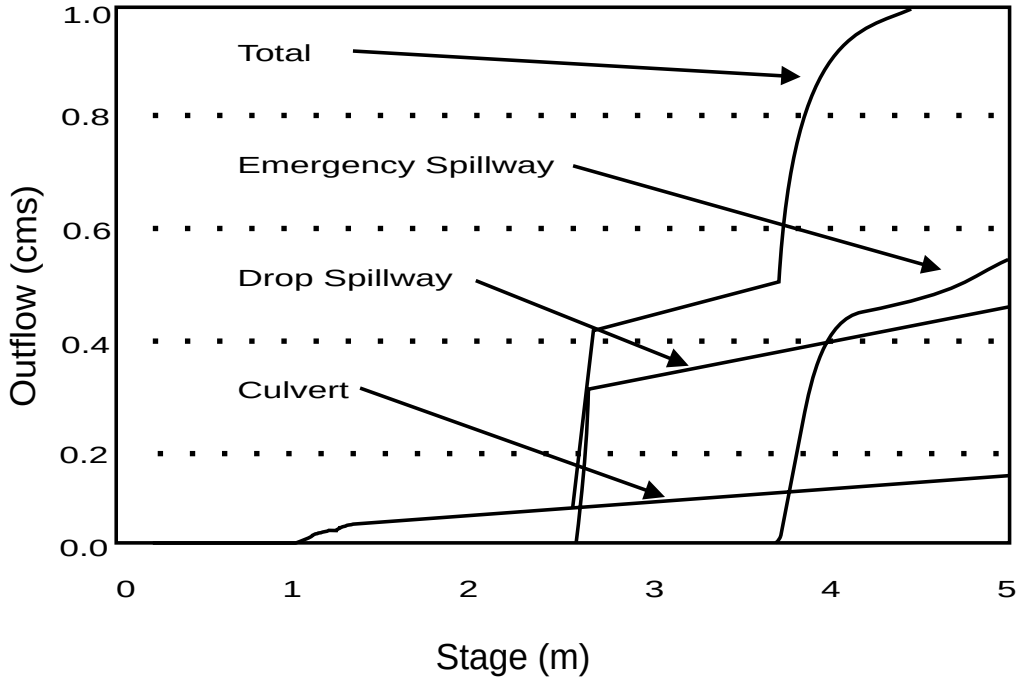

Figure 14.3.2. Stage-discharge relationship for individual structures and all structures combined including transitions between flow regimes.

Each of the possible outlet structures has at least two possible flow regimes, either no flow (when the type structure is not present or the water surface stage is below the outlet structure stage) or flow (when there is outflow through the structure). The porous structures (rock-fill, filter fence, and straw bales) have three possible flow regimes: no flow, flow through the structure, and flow overtopping the structure. Flow is said to transition from one flow regime to another. These transitions occur at specific water surface stages for each structure. Thus, as the water surface stage rises or falls through a transition, the outflow function, $f_{Qo}(H)$, must change.

If more than one outlet structure is present, the transitions for each structure must be combined together. Consider the case of a large farm pond with a culvert outlet for small flows, a drop spillway for large storms, and an emergency spillway to prevent breaching of the dam, as illustrated in Fig. 14.3.1. Each structure has a transition from no flow to flow at a different stage. The overall outflow function, $f_{Qo}(H)$, must reflect all three transitions as seen in Fig. 14.3.2.

Equations used in developing the stage-discharge relationships are discussed in the following section.

14.3.1 Drop-Inlet Spillway

A drop-inlet spillway is a common outflow structure used in farm ponds and sediment detention basins. It consists of a vertical riser connected to a horizontal or near horizontal barrel. The drop spillway has two possible outflow regimes; no flow and flow. If the water-surface stage is below the level of the riser opening, the outflow is zero. Flow through a drop spillway occurs when the water surface stage is above the riser inlet. The outflow rate is determined by assuming weir flow, orifice flow, and pipe flow control. The outflow rate is the minimum of the three possible controlling flows.

The discharge over a sharp-crested weir is related to the driving head by the sharp-crested weir equation (Haan et al., 1994; SCS, 1984; and Schwab et al., 1981):

$$Q_{weir} = C_{weir} L H^{\frac{3}{2}} \qquad [14.3.1]$$

where Q_{weir} is the discharge ($ft^3 \cdot s^{-1}$), C_{weir} is the weir coefficient ($ft^{0.5} \cdot s^{-1}$), L is the length of the weir (ft) (circumference of the riser), and H is the driving head (ft). For risers, C_{weir} is generally between 3.0 and 3.2. The discharge through an orifice can be determined with the orifice equation (Haan et al., 1994; SCS, 1984; and Schwab et al., 1981):

$$Q_{orifice} = C' A_o \sqrt{2\, g\, H} \qquad [14.3.2]$$

where C' is the dimensionless orifice coefficient, A_o is the cross-sectional area of the orifice (ft^2) (flow area of the riser), g is the gravitational constant (32.2 $ft \cdot s^{-2}$), and H is the head on the orifice (ft). For a riser inlet, C' is typically 0.6.

The discharge through a pipe flowing full is determined from the following equation (Haan et al., 1994; SCS, 1984; and Schwab et al., 1981):

$$Q_{pipe} = \frac{A_p \sqrt{2\, g\, H'}}{\sqrt{1 + K_e + K_b + K_c L}} \qquad [14.3.3]$$

where A_p is the cross-sectional flow area of the pipe (ft^2), H' is the driving head ft, K_e is the dimensionless entrance head loss coefficient, K_b is the dimensionless bend loss coefficient, K_c is the

friction loss coefficient (ft^{-1}), and L is the length of the pipe (including the riser) (ft). The dissipation of energy due to entrance losses is accounted for by K_e with a typical value of 1.0. The energy dissipation caused by the bend where the barrel meets the riser is accounted for by K_b. For a drop inlet with a single sharp bend, K_b is 0.5. The energy dissipation due to friction is accounted for by $K_c L$; where K_c is a parameter dependent upon the size and roughness of the conduit. Flow through the drop spillway is the minimum of the three possible controlling flows:

$$Q_{drop\ spillway} = MIN(Q_{weir}, Q_{orifice}, Q_{pipe}) \qquad [14.3.4]$$

14.3.2 Perforated Riser

Perforated risers are often used as outlet structures for terrace systems. A perforated riser is similar to a drop inlet in that both employ a riser that empties into a subsurface conduit. The perforated riser includes slots along the riser to allow complete drainage of the terrace, and a bottom orifice plate to limit flow to the subsurface conduit located below the slots. The perforated riser has three possible outflow regimes: no flow, flow through the side slots, and flow submerging the perforated riser. If the water surface stage is below the level of the bottom of the slots, the outflow is zero. A schematic for a perforated riser is given in Fig. 14.3.3.

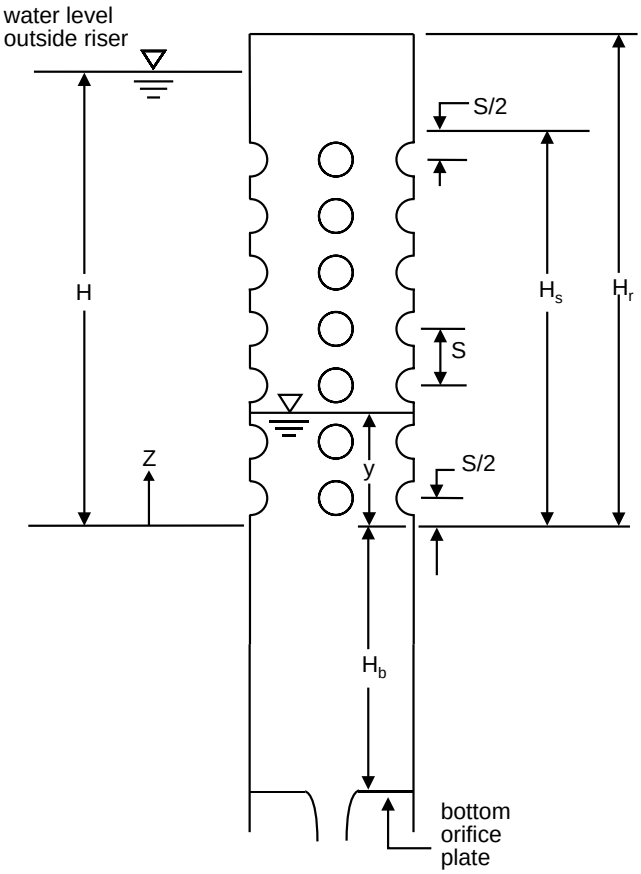

Figure 14.3.3. Schematic of a perforated riser.

When the water surface stage moves above the level at the bottom of the slots, water begins to flow through the riser. Flow can be controlled by either the slots (slot flow), the orifice plate located below the slots (orifice flow), or by the subsurface conduit flowing in full pipe flow (pipe flow). The outflow rate is determined by computing the slot flow, orifice flow, and the pipe flow and taking the minimum controlling flow.

Flow through slots can be defined by equations developed by McEnroe et al. (1988), but these relationships are implicit, requiring trial and error solutions. In WEPPSIE, a regression relationship was developed to compute flow through the slots using stage-discharge points computed according to the McEnroe et al. (1988) procedure. The following functional relationship between driving head and outflow was chosen because it had the best average r^2 of 0.991:

$$Q_{slots} = \frac{1}{A_{PR} + \frac{B_{PR}}{H^{1.5}}} \qquad [14.3.5]$$

where Q_{slots} is the outflow ($ft^3 \cdot s^{-1}$), H is the driving head (ft) (water surface stage - stage of the bottom of the slots), and A_{PR} ($ft^{-3} \cdot s$) and B_{PR} ($ft^{-2.5} \cdot s$) are regression coefficients. A_{PR} and B_{PR} are unique for each user-defined perforated riser and are determined using stage-discharge points computed in the front-end interface according to the McEnroe et al. (1988) procedure. To determine flow controlled by the bottom orifice plate, Eq. [14.3.2] is utilized with the stage and flow area of the bottom orifice plate. Equation [14.3.3] is used with the dimensions of the subsurface conduit to determine flow controlled by pipe flow in the subsurface conduit. The outflow contribution by a perforated riser is the minimum controlling flow:

$$Q_{perforated\ riser} = MIN(Q_{slots}, Q_{orifice}, Q_{pipe}) \qquad [14.3.6]$$

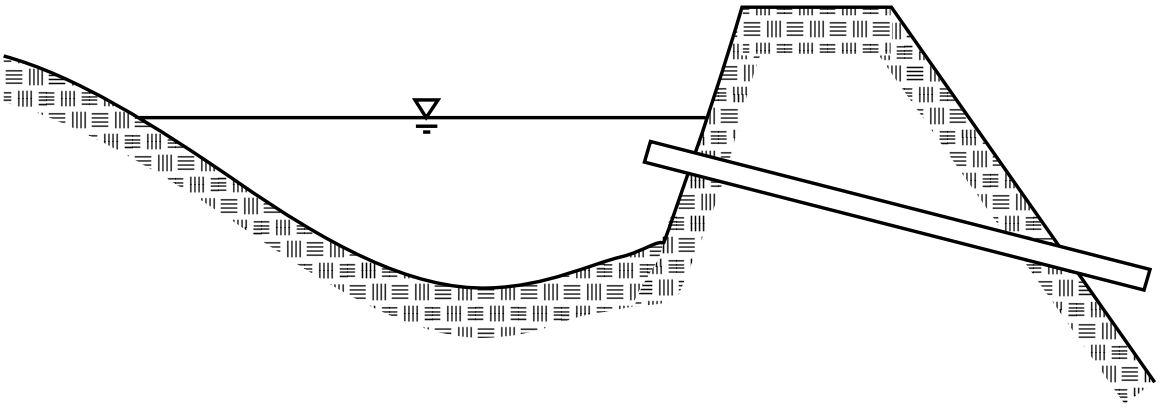

Figure 14.3.4. Schematic of a trickle tube.

14.3.3 Culverts

Culverts, sometimes called trickle tube spillways, can be used as outlet structures for farm ponds and sediment basins as shown in Fig. 14.3.4. Culverts are also used to control flows under roadways, often resulting in an impoundment formed from ponding upstream of the culvert. Discharge through a culvert is dependent upon many factors: upstream depth, downstream depth, culvert length, size, roughness, slope, entrance characteristics, and exit characteristics. In WEPPSIE, culverts have two

possible flow regimes; no flow and flow. If the water surface stage is below the level of the culvert inlet the outflow is zero, otherwise there is flow through the culvert.

Table 14.3.1. Constants for inlet control culvert discharge equations.

Shape and Material	Inlet Description	K	M	c	Y
Rectangular Box	45 deg. wingwall flare d = 0.043D	0.510	0.667	0.0309	0.80
	18 to 33.7 deg. wingwall flare d = 0.083D	0.486	0.667	0.0249	0.83
Rectangular Box	90 deg. headwall w/0.75" chamfers	0.515	0.667	0.0375	0.79
	90 deg. headwall w/45 deg. bevels	0.495	0.667	0.0314	0.82
	90 deg. headwall w/33.7 deg. bevels	0.486	0.667	0.0252	0.865
Rectangular Box	0.75" chamfers; 45 deg. skewed headwall	0.522	0.667	0.0402	0.73
	0.75" chamfers; 30 deg. skewed headwall	0.533	0.667	0.0425	0.705
	0.75" chamfers; 15 deg. skewed headwall	0.545	0.667	0.0451	0.68
	45 deg. bevels; 10 to 45 deg. skewed headwall	0.498	0.667	0.0327	0.75
Rectangular Box	45 deg. non-offset wingwall flares	0.497	0.667	0.0339	0.803
	0.75" chamfers; 18.4 deg. non-offset wingwall flares	0.493	0.667	0.0361	0.806
	18.4 deg. non-offset wingwall flares; 30 deg. skewed barrel	0.495	0.667	0.0386	0.71
Rectangular Box Top Bevels	45 deg. wingwall flares - offset	0.497	0.667	0.0302	0.835
	33.7 deg. wingwall flares - offset	0.495	0.667	0.0252	0.881
	18.4 deg. wingwall flares - offset	0.493	0.667	0.0227	0.887
Circular	Smooth tapered inlet throat	0.534	0.555	0.0196	0.89
	Rough tapered inlet throat	0.519	0.640	0.0286	0.9
Elliptical Inlet Face	Tapered inlet - beveled edges	0.536	0.622	0.0368	0.83
	Tapered inlet - square edges	0.504	0.719	0.0478	0.80
	Tapered inlet - thin edge projecting	0.547	0.800	0.0598	0.75
Rectangular	Tapered inlet throat	0.475	0.667	0.0179	0.97
Rectangular Concrete	Side tapered - less favorable edges	0.560	0.667	0.0466	0.85
	Side tapered - more favorable edges	0.560	0.667	0.0378	0.87
Rectangular Concrete	Slope tapered - less favorable edges	0.500	0.667	0.0466	0.65
	Slope tapered - more favorable edges	0.500	0.667	0.0378	0.71

The determination of outflow through the culvert is based upon the FHA (1985) methodology. Outflow through the culvert is determined by computing the outflow if the inlet is unsubmerged, inlet is submerged, and if the culvert is flowing under full pipe flow. The outflow is the minimum controlling flow. When the inlet is unsubmerged, discharge is determined by (FHA, 1985):

$$\frac{HW_i}{D_{culvert}} = K\left[\frac{Q_{unsubmerged}}{A_{cs}D^{0.5}}\right]^M \qquad [14.3.7]$$

where HW_i is the headwater depth (ft), $D_{culvert}$ is the interior height of the culvert (ft), $Q_{unsubmerged}$ is the discharge ($ft^3 \cdot s^{-1}$), A_{cs} is the cross-sectional area of the culvert barrel (ft^2), and K and M are constants given in Table 14.3.1. When the inlet is submerged, discharge is computed from (FHA, 1985):

$$\frac{HW_i}{D} = c\left(\frac{Q_{submerged}}{AD^{0.5}}\right)^2 + Y - 0.5\,S \qquad [14.3.8]$$

where c and Y are constants, given in Table 14.3.1 and S is the culvert barrel slope ($ft \cdot ft^{-1}$). Full pipe flow is determined according to Eq. [14.3.3]. The contribution to the total outflow by a culvert is the minimum controlling flow:

$$Q_{culvert} = MIN\left(Q_{unsubmerged}, Q_{submerged}, Q_{pipe}\right) \qquad [14.3.9]$$

In practice it is common for engineers to use two or more identical culverts to route channels under roadways. It is also possible for engineers to utilize two culverts of different shapes, sizes, or at different elevations. To accommodate these situations, the impoundment element allows the user to specify two different sets of any number of identical culverts.

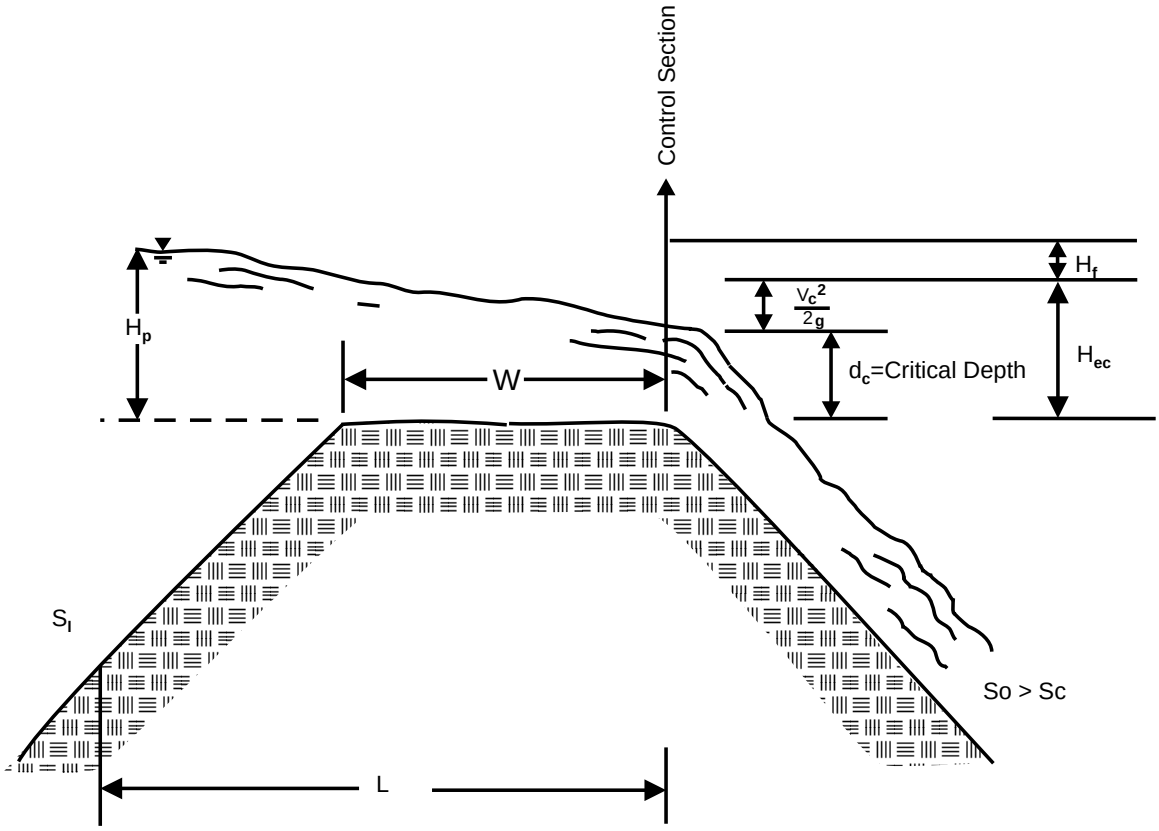

Figure 14.3.5. Schematic of an emergency spillway showing a control section.

14.3.4 Emergency Spillways and Open Channels

In many larger farm ponds and sedimentation basins, emergency spillways are used to route the excess runoff from very large storm events that cannot be routed through the principle spillway in order to keep the excess flow from overtopping and breaching an earthen dam. Sometimes an open channel forms the only outlet structure. Emergency spillways and open channel outlet structures have two

possible flow regimes; either no flow or flow. If the water surface stage is below the level of the open channel inlet the outflow is zero.

To save computational time, flow through an open channel $Q_{openchannel}$ $(ft^3 \cdot s^{-1})$is determined with a fourth-order polynomial expression:

$$Q_{open\ channel} = A + BH + CH^2 + DH^3 + EH^4 \qquad [14.3.10]$$

where H is the driving head (water surface stage - stage of the open channel inlet) (*ft*) and *A*, *B*, *C*, *D*, and *E* are coefficients unique to the user-defined open channel outlet. For the set of emergency spillway dimensions specified for a given outlet, a stage-discharge data set is computed with the steady-state standard step method (Fogle and Barfield, 1992; Chow, 1959). This data set is utilized with the regression routines in the interface to compute the coefficients *A*, *B*, *C*, *D*, and *E*.

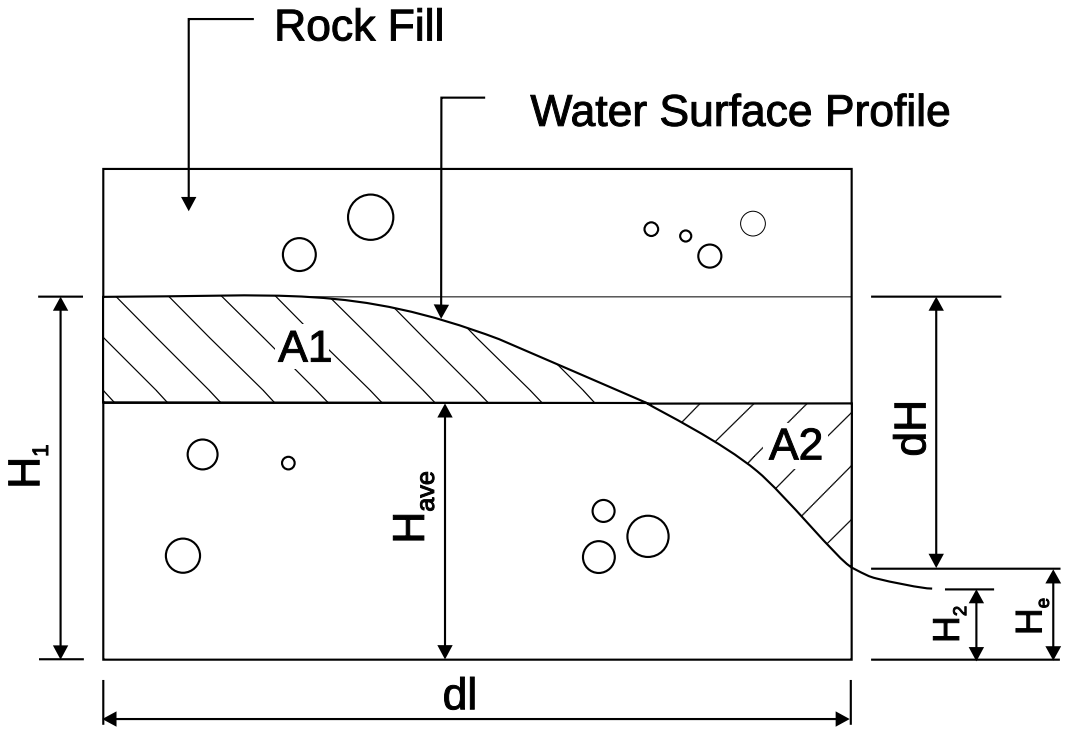

Figure 14.3.6. Schematic of a rock-fill check dam.

14.3.5 Rock-Fill Check Dams

Construction, mining, and silviculture operations need inexpensive temporary sediment traps. Porous-rock-fill check dams provide an inexpensive, easily-constructed solution. A porous-rock-fill check dam is simply a pile of rocks obstructing the free flow of sediment-laden water. Frequently a rock-fill check dam is constructed with a coarse sand or fine gravel core in order to trap the most sediment. This core is typically covered by a larger rip-rap to prevent washout. A schematic of a porous-rock-fill dam is given in Fig. 14.3.6. Further references to this structure will be as a ditch check. The units in this section are metric in keeping with the regression equations available for predicting flow though rock fill.

A ditch check dam has three possible outflow regimes; no flow, flow through the rock, or a combination of flow overtopping the structure and flow through the rock. If the water surface stage is below the level of the rock-fill inlet the outflow is zero.

Flow begins when the water surface stage rises above the level of the rock-fill inlet. Flow through the rock is determined using a numerical adaptation of the graphical method developed by Haan et al. (1994):

$$Q_{rock-fill} = wd_{rf}\left(\frac{dH}{a\ dl}\right)^{1/b} \qquad [14.3.11]$$

where $Q_{rock-fill}$ is the flow rate through the check dam ($m^3 \cdot s^{-1}$) wd_{rf} is the width of the rock-fill (m), dH is the head loss through the rock-fill (m), dl is the length of the rock-fill (m), and a and b are coefficients given graphically in Haan et al. (1994). Regression equations were determined for the coefficients, using data points taken from the Haan et al. (1994) graph. Coefficient a is determined by either interpolation or extrapolation between the following equations using the size of the rocks and the flow length:

$$\begin{aligned} L_{RF} &= 0.5\ m & a &= 3.04185\ dia_{RF}^{-0.34677} \\ L_{RF} &= 1.0\ m & a &= 1.91041\ dia_{RF}^{-0.34935} \\ L_{RF} &= 2.0\ m & a &= 1.19637\ dia_{RF}^{-0.35422} \\ L_{RF} &= 3.0\ m & a &= 0.90990\ dia_{RF}^{-0.35705} \end{aligned} \qquad [14.3.12]$$

where L_{RF} is the flow length through the rock-fill (m) and dia_{RF} is the average rock diameter (m). The coefficient b is determined using the size of the rocks, or:

$$b = \frac{1}{1.50056 - 0.0001317\dfrac{\log(dia_{RF})}{dia_{RF}}} \qquad [14.3.13]$$

When flow overtops the rock-fill, the overtopping flow is modeled as a broad crested weir and added to the flow through the rock-fill (Haan et al., 1994):

$$Q_{rock\ fill} = wd_{rf}\left(\left(\frac{dH}{a\ dl}\right)^{1/b} + 0.519(H - H_{ot})^{1.5}\right) \qquad [14.3.14]$$

where 0.519 is the broad crested weir coefficient ($m^{0.5} \cdot s^{-1}$) and H_{ot} is the stage at which the rock-fill is overtopped.

14.3.6 Filter Fence and Straw Bale Check Dams

Check dams can also be constructed with straw bales or filter fence. Both straw bale and filter fence check dams provide inexpensive, easily-constructed sediment trapping structures. The discharge through a filter fence or straw bale check dam is dependent upon the slurry flow rate, flow stage, and cross-sectional flow area. A filter fence or straw bale check dam has three possible outflow regimes: no flow, flow through the filter, or flow overtopping the structure and flow through it. *Although WEPPSIE will compute flow overtopping a filter fence or a straw bale check dam, in reality most filter fence or straw bale check dams will wash out under such large flows.* If the water surface stage is below the level of the filter fence or straw bales inlet, the outflow is zero.

Flow begins when the water surface stage rises above the level of the check dam inlet. The slurry flow rate can be utilized to compute the flow through a straw bale or a filter fence check dam by assuming a rectangular cross-sectional flow area (Haan et al., 1994):

$$Q_{filter\ fence\ or\ straw\ bale} = V_{sl}\ b\ H \qquad [14.3.15]$$

where $Q_{filter\ fence\ or\ straw\ bale}$ is flow rate ($ft^3 \cdot s^{-1}$) V_{sl} is the slurry flow rate ($ft \cdot s^{-1}$), W_b is the bottom width (ft), and H is the stage (ft).

When flow overtops a filter fence, the overtopping flow is modeled as a sharp crested weir and added to the flow through the filter fence given in Eq. [14.3.15], or:

$$Q_{filter\ fence} = wd_{ff} \left[V_{sl}\ (H - H_{ff}) + \left(3.27 + \frac{0.4(H - H_{ot})}{(H_{ot} - H_{ff})} \right) (H - H_{ot})^{1.5} \right] \qquad [14.3.16]$$

where wd_{ff} is the width of the filter fence (ft), V_{sl} is the slurry flow rate ($ft \cdot s^{-1}$), H is the water surface stage (ft), H_{ff} is the inlet stage (ft), H_{ot} is the overtop stage (ft).

When flow overtops a straw bale check dam, the overtopping flow is modeled as a broad crested weir and added to the flow through the straw bales given in Eq. [14.3.15]:

$$Q_{straw\ bale} = wd_{sb} \left[V_{sl}\ (H - H_{sb}) + 3.087\ (H - H_{ot})^{1.5} \right] \qquad [14.3.17]$$

where wd_{sb} is the width of the straw bales (ft), V_{sl} is the slurry flow rate ($ft \cdot s^{-1}$), H is the water surface stage (ft), H_{sb} is the inlet stage (ft), and H_{ot} is the overtop stage (ft).

When the flow overtops a filter fence or a straw bale check dam, the structure will probably wash out. Filter fences and straw bale check dams are designed to filter low flows and should not see water surface stages greater than 0.2 to 0.4 meters. WEPPSIE assumes that proper maintenance is utilized to promptly repair any damaged check dam. When choosing slurry flow rates the user should consider the effects of sediment-laden water and clogging which usually result in lower slurry flow rates as compared to clear water.

14.3.7 User-Defined Stage-Discharge Relationship

A user-defined stage discharge relationship is utilized when a structure is encountered that is not included in the user interface. When using a user-defined stage-discharge relationship, two flow regimes are possible. When the water surface stage is below the user-defined stage at which flow starts, the outflow is zero. When the water surface stage is above the stage at which flow starts, flow is computed according to the fourth-order polynomial given in Eq. [14.3.10].

To determine the coefficients of Eq. [14.3.10], the user enters as many stage-discharge points as possible (at least 15). Regression routines (Press et al., 1986) are then utilized to determine the coefficients in Eq. [14.3.10]. Fifteen points are recommended to ensure that the stage-discharge relationship predicted by the fourth-order regression has no unexpected dips. Further, those fifteen points should be fairly evenly spaced within the range of possible stages.

To save computational time, the user-defined stage-discharge relationship utilizes the same fourth-order polynomial function used for emergency spillway/open channel flow. Thus, the user is limited to using either points from a user-defined stage-discharge relationship or points determined with the emergency spillway/open channel flow water surface profile routine in determining the coefficients for the fourth-order polynomial.

14.3.8 Overall Outflow Expression

The total outflow is simply the summation of the outflow contribution of every possible structure making it possible to have any combination of the possible outflow structures on a given impoundment (see Figs. 14.3.1 and 14.3.2). If a structure is not present or the water surface stage is below an outlet structure's inlet stage, its contribution to the total outflow is zero. If the water surface stage is above an outlet structure's inlet stage, it contributes to the total outflow. The total outflow is determined by summing the contributions of each possible outlet structure considering the relationship of the stage to the transition stages for each of the possible outlet structures. The total outflow is determined with the following expression:

$$\begin{aligned} Q_{total} = {} & Q_{drop\ spillway} \\ & + Q_{perforated\ riser} \\ & + Q_{culvert\ set\ 1} \\ & + Q_{culvert\ set\ 2} \\ & + Q_{emergency\ spillway,\ open\ channel,\ user-defined} \\ & + Q_{rock\ fill} \\ & + Q_{filter\ fence,\ straw\ bale} \end{aligned} \qquad [14.3.18]$$

14.4 Stage-Area Relationship

The stage-area relationship, $f_A\,(H)$, utilized in the continuity expression, Eq. [14.2.5], is in the form of a power function as recommended by Laflen (1972), Haan and Johnson (1967), and Rochester and Busch (1974). The functional relationship between area and stage is given in the following expression:

$$A_{imp} = f_A\,(H) = a + bH^c \qquad [14.4.1]$$

where H is the stage (ft) and a, b, and c are coefficients. To determine the coefficients in Eq. [14.4.1], the user enters as many stage-area points as possible (at least 10), and regression routines (Press et al., 1986) are used to determine the coefficients a, b, and c. Ten points are recommended to ensure that the stage-area relationship predicted by the power function provides a reasonable estimation of the actual stage-area relationship.

14.5 Evaporation and Infiltration

On a daily basis the impoundment stage is adjusted for evaporation and infiltration losses. Evaporative losses, $evap$ ($mm \cdot d^{-1}$), are computed from the potential evapotranspiration, PET ($mm \cdot d^{-1}$), computed elsewhere in the WEPP code according to (Kohler et al., 1955):

$$evap = 0.7\ PET \qquad [14.5.1]$$

The coefficient of 0.7 was given by Kohler et al. (1955) for small lakes and ponds.

Infiltration losses, $infil$ ($mm \cdot d^{-1}$), are computed using:

$$infil = K_{sat}\ T_{day} \qquad [14.5.2]$$

K_{sat} is the saturated hydraulic conductivity of the layer draining the impoundment ($mm \cdot h^{-1}$), and T_{day} is

24 hours. Engineering judgement is required on the part of the user to choose a reasonable value of K_{sat} for a given situation. For impoundments with a relatively homogeneous subsurface such that drainage is vertical, the layer with the lowest K_{sat} is considered the limiting layer, and it's K_{sat} is used. For impoundments with a heterogeneous subsurface, such as a sandy soil above a clay base, the K_{sat} for the sandy soil is utilized because it is the draining layer. At the end of each day the stage is adjusted for evaporation and infiltration according to:

$$H_{new} = H - (evap - infil) / 304.8 \qquad [14.5.3]$$

where H_{new} is the stage at the end of the day (*ft*), and H is the starting stage (*ft*).

14.6 Sedimentation

The hydraulic simulation section of WEPPSIE performs a direct numerical integration of an expression of continuity. A temporary file is created of the predicted outflow hydrograph including stage and outflow at each time step. The sedimentation simulation section of the impoundment element determines the amount of sediment deposited and the outflow concentration for each time step. Deposition and effluent sediment concentration are predicted using conservation of mass and overflow rate concepts. When outflow ends, settling in the permanent pool is determined using quiescent settling theory.

Sediment inputs, as dictated by the WEPP convention, include total inflow suspended sediment concentration, percent of sediment in each size class (clays, silts, sands, small aggregates, and large aggregates), and the mean particle size diameter, d_{50}, for each size class. Size class divisions are based upon the CREAMS criteria (Foster et al., 1985; USDA, 1980). WEPPSIE must return outputs similar to the inputs for further routing through a watershed. The impoundment element also outputs a detailed analysis of incoming and effluent sediment amounts and concentrations for each particle size class.

The goal of the sedimentation algorithm is to determine sediment concentration exiting the impoundment at the end of each time step taken in the hydraulic simulation. One approach to this problem would have been to use an existing validated prediction model such as DEPOSITS (Ward et al., 1979), CSTRS (Wilson and Barfield, 1984), or BASIN (Wilson and Barfield, 1985). The computational requirements of these models are, however, too time-consuming to use for daily predictions over a twenty year WEPP model simulation period. Thus, a simpler algorithm is needed that predicts values reasonably close to the more complex models. The CSTRS model of Wilson and Barfield (1984) was chosen over the other models as the standard of comparison due to its prediction accuracy, ability to evaluate the effects of mixing, and simplicity of inputs.

14.6.1 Conservation of Mass

The simplified sedimentation algorithms developed for WEPPSIE are based upon the principle of conservation of mass, as applied to a single continuously-stirred reactor or:

$$\frac{dM}{dt} = Q_i\, C_i - Q_o\, C_o - \frac{d\ Dep}{dt} \qquad [14.6.1]$$

where *dM/dt* is the change in total mass in the impoundment over time ($lbs \cdot s^{-1}$), Q_i is inflow rate ($ft^3 \cdot s^{-1}$), Q_o is the outflow rate ($ft^3 \cdot s^{-1}$), C_i is the incoming sediment concentration ($lbs \cdot ft^{-3}$), C_o is the outgoing sediment concentration ($lbs \cdot ft^{-3}$), and *Dep* is the deposition (*lbs*). The mass of sediment in the impoundment, *M* (*lbs*), is equal to $C_{avg}Vol$ where C_{avg} is the average concentration in the impoundment ($lbs \cdot ft^{-3}$), and *Vol* is the volume of the impoundment (ft^3). If the assumption is made that the pond can be represented as a single continuously-stirred reactor, then the average concentration is equal to the

outflow concentration, C_o. Using dye tracers, Griffin et al. (1985) showed that two continuously-stirred reactors in series (CSTRS) were the optimum model to represent small ponds; however, the data also showed that one continuously-stirred reactor was a reasonable representation (Griffin, 1983). Using the assumption that the impoundment can be represented as a single continuously-stirred reactor, the mass in suspension in the impoundment, M, is equal to $C_o\forbar{V}$. Through a series of mathematical manipulations, Eq. [14.6.1] can be solved numerically to determine the outgoing sediment concentration at the end of a given time step, or:

$$C_{on} = \frac{Q_i\, C_i\, \Delta t - Dep + C_o\left(\frac{\forbar{V} + \forbar{V}_n}{2} - \frac{Q_i\, \Delta t}{2}\right)}{\frac{\forbar{V} + \forbar{V}_n}{2} + \frac{Q_i\, \Delta t}{2}} \qquad [14.6.2]$$

where C_{on} is the outgoing sediment concentration at the end of the time step ($lbs \cdot ft^{-3}$) Δt is the length of the time step (s), C_o is outgoing sediment concentration at the beginning of the time step, $\forbar{V}$ and $\forbar{V}_n$ are the volume of the pond at the beginning and end of the time step (ft^3) respectively, and the rest of the terms are as defined for Eq. [14.6.1]. The accuracy of Eq. [14.6.2] is dependent upon an accurate determination of deposition since the other terms are known from the hydraulic simulation or the previous time step.

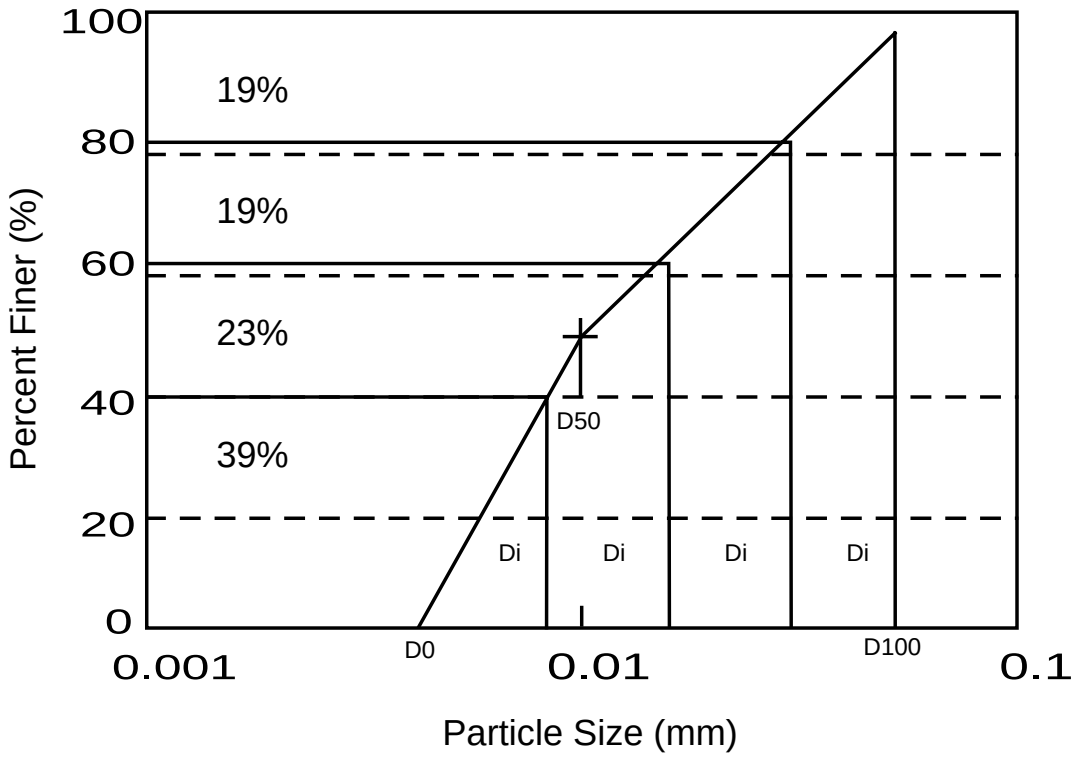

Figure 14.6.1. Division of particle size distribution into four subclasses.

To represent sedimentation more accurately the five sediment size classes are split into several subclasses and Eq. [14.6.2] is utilized to determine a C_{on} for each subclass. At the beginning of the simulation, the number of subclasses for each particle size class, ranging from two to ten, is defined by the user. In the front-end interface section of the routines, each size class is evenly divided into the user-

defined number of subclasses based upon the logarithmic particle size range. The daily input of sediment in each particle size class is divided into the portion in each size subclass using the log-mean particle size diameter for the size class as seen in Fig. 14.6.1. Throughout the entire simulation, the concentration of sediment in each particle size subclass is maintained. Runs were made with two to ten particle size subclasses. Little improvement in accuracy was noted with more than six particle size subclasses, and considering the simplifying assumptions going into the WEPP convention, two to four particle size subclasses provides sufficient accuracy.

14.6.2 Deposition

When the impoundment has inflow, sediment deposition for each particle subclass is based upon an analogy to the overflow rate concept (Barfield et al., 1981; Haan et al., 1994). The overflow rate concept linearly relates deposition to the ratio of the settling velocity of the sediment particle to the overflow rate, defined as:

$$V_c = \frac{Q_o}{A} \qquad [14.6.3]$$

where V_c is the overflow rate ($ft \cdot s^{-1}$), Q_o is the outflow rate ($ft^3 \cdot s^{-1}$), and A is the impoundment area (assumed constant) (ft^2). The particle settling velocity, V_s ($ft \cdot s^{-1}$), is determined from discrete settling theory using Stoke's law for small silts and clays or empirical data for large particles. If V_c is less than V_s, then 100% of the suspended sediment settles out of suspension. If V_c is greater than V_s, then the ratio, V_s/V_c, of the suspended sediment settles out of suspension (Haan et al., 1994). The overflow rate is actually the settling velocity of a particle that can just settle to the bottom of a reservoir during its flow through time. In addition to being defined by Q_o/A, it can be expressed in terms of detention times as:

$$V_c = \frac{H}{t_D} \qquad [14.6.4]$$

where H is the settling depth (ft) and t_D is the detention time (s). The settling velocity can be idealized as:

$$V_s = \frac{H}{t_{D\,100}} \qquad [14.6.5]$$

where $t_{D\,100}$ is the detention time required for 100% of the particles with settling velocity V_s to settle out. Thus, V_s/V_c can be conceptualized as:

$$\frac{V_s}{V_c} = \frac{\frac{H}{t_{D\,100}}}{\frac{H}{t_D}} = \frac{t_D}{t_{D\,100}} \qquad [14.6.6]$$

which is the ratio of the actual detention time to the detention time required for 100% of the sediment to settle out of suspension. The deposition routine in the WEPP impoundment element utilizes Eq. [14.6.6] with modifications defined below.

For each time step, the deposition routine begins with the computation of the detention times. The actual detention time is based upon the ratio of the impoundment volume to the outflow rate:

$$t_D = \frac{(C_t\ (1 - DS)\ Vol)}{Q_o} \qquad [14.6.7]$$

where t_D is detention time (s), C_t is an empirical parameter to account for impoundment geometry, hydraulic response, and stratification of the suspended sediment, *DS* is the dead storage (the portion of the pond area that does not contribute to settling) (Griffin et al., 1985), *Vol* is the average impoundment volume over the time step (ft^3). and Q_o is the average outflow rate over the time step ($ft^3 \cdot s^{-1}$). The detention time required for 100% of the suspended sediment to settle out of suspension is computed from the average impoundment depth (volume / area) and the settling velocity, or:

$$t_{D\,100} = \frac{(1 - DS)\ \dfrac{Vol}{\bar{A}}}{V_s} \qquad [14.6.8]$$

where $\bar{A}$ is the average impoundment area over the time step (ft^2), and V_s is the settling velocity for the given sediment particle size. Since the impoundment element utilizes five sediment size classes and up to ten subclasses for each size class, all with unique settling velocities, $t_{D\,100}$ must be computed for each particle size subclass.

In the computation of both t_D and $t_{D\,100}$, the concept of dead storage is utilized. According to Griffin et al. (1985), dead storage is related to the ratio of impoundment length (in the flow direction) to impoundment width. Long impoundments with length to width ratios greater than two have approximately 15% dead storage on average while short impoundments with length to width ratios less than two have more dead storage, approximately 25% on average (Griffin et al., 1985). The impoundment length is determined with a power function, or

$$L = a_L + b_L\ H^{c_L} \qquad [14.6.9]$$

where L is the impoundment length (*ft*), H is the water surface stage (*ft*), and a_L, b_L, and c_L are the power function coefficients. The power function in Eq. [14.6.9] is developed in the front-end interface section of the program from a number of stage-length points entered by the user. The equation is similar to the stage-area power function. The width is determined by dividing the area by the length. For length to width ratios less than two, the dead storage is set equal to 0.25; For length to width ratios greater than two, the dead storage is set equal to 0.15 based on the Griffin et al. (1985) studies.

Once the detention times are determined, the actual deposition occurring within each size subclass during the time step Δt must be determined. Two different deposition rate expressions are used, depending on the time period during the runoff event. Figure 14.6.2 illustrates the times during which each deposition expression is applied. One expression is used throughout the duration of the inflow hydrograph, based upon the inflow rate and incoming sediment concentration, or:

$$\frac{d\ Dep}{dt} = \left(\frac{t_D}{t_{D\,100}} \right) Q_i\ C_i\ \Delta t \qquad [14.6.10]$$

where *Dep* is the cumulative deposition (*lbs*), $Q_i C_i \Delta t$ is the inflow mass of sediment during the time period, and $t_D/t_{D\,100}$ represents the fraction of the inflow mass trapped.

After inflow ceases, the deposition rate is determined from quiescent settling theory with the sediment concentration in the pond and the particle settling velocity, or:

$$\frac{d\ Dep}{dt} = c_d \left(\frac{t_D}{t_{D\,100}} \right) C_o\ V_s\ A\ \Delta t \qquad [14.6.11]$$

where c_d is a parameter to account for impoundment geometry, hydraulic response, and stratification of the suspended sediment, and C_o is the outgoing sediment concentration at the beginning of the time step. $C_o V_s A \Delta t$ is the mass in the impoundment that would settle out if the concentration in the impoundment were uniform, and $c_d(t_D/t_{D\,100})$ is the fraction that corrects for nonuniformity. Once the deposition rate is determined, it is used in Eq. [14.6.2] to determine the effluent sediment concentration for each particle size subclass. This sediment concentration then becomes the sediment concentration at the beginning of the next time step and the process is repeated to "march" through the hydrograph.

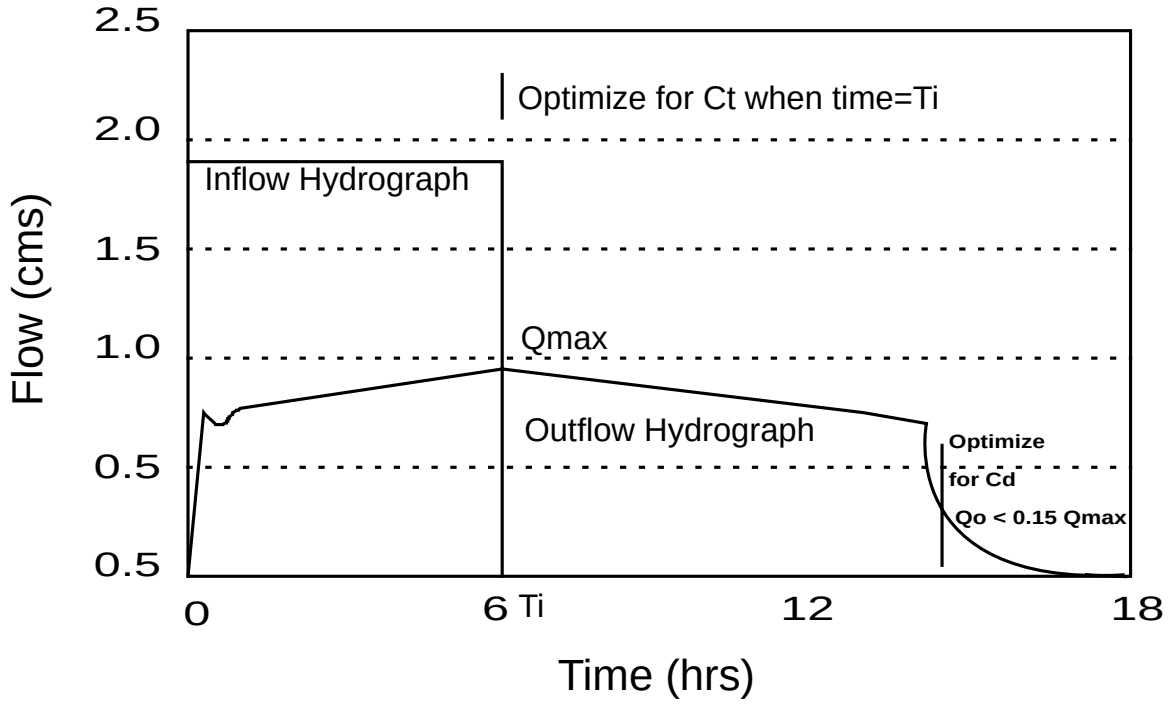

Figure 14.6.2. Times for which each deposition routine is used (after Lindley et al., 1993).

This deposition methodology includes two calibration coefficients, c_t and c_d, that are used to account for the effects of impoundment geometry and hydraulic response. Regression equations that utilize hydraulic and geometric parameters known from the hydraulic simulation performed before the sedimentation routines begin are used to estimate c_t and c_d. These regression coefficients were developed from a database generated with the CSTRS model using impoundments with a variety of shapes, sizes, and outflow structures ranging from small check dams without a permanent pool to large farm ponds with a permanent pool. Using the CSTRS model as a standard, optimal values of c_t and c_d were determined. From these optimal values and data on the impoundment geometry and hydraulic routing, estimation models for c_t and c_d were developed. In order to better estimate c_t and c_d, impoundments are split into two groups: 1) small impoundments without a permanent pool including terraces, rock-fill check dams, filter fence, and straw bale check dams; and 2) large impoundments with a permanent pool such as farm ponds. A description of the variables used in the c_t and c_d estimation models are presented in Table 14.6.1. The estimation models for small impoundments are presented in Table 14.6.2 and models for large impoundments are presented in Table 14.6.3.

Table 14.6.1. Variables considered for inclusion in c_t and c_d estimation models.

Variable	Definition	Units
VI	Volume of the inflow storm event	ft^3
VPI	Volume of the pond at the average stage, *HI* (averaged over the duration of the inflow hydrograph)	ft^3
VMX	Volume of the pond at the maximum stage	ft^3
VMXVI	VMX/VI. Ratio of the volume of the pond at the maximum stage to the volume of the inflow storm event (*dimensionless*)	
AR	Area of the pond at the riser	ft^2
AI	Area of the pond at the average stage (averaged over the duration of the inflow hydrograph)	ft^2
QO	Outflow corresponding to the average stage, HI (averaged over the duration of the inflow hydrograph)	$ft^3 \cdot s^{-1}$
VS	Particle settling velocity (from Stoke's Law or empirical data)	$ft \cdot s^{-1}$
QOAIVS	(QO/AI)/VS; ratio of the overflow rate to the settling velocity	*dimensionless*
QOARVS	(QO/AR)/VS; ratio of the overflow rate to the settling velocity	*dimensionless*
QOAIVSE	(1 - exp(-((QO/AI)/VS)))	*dimensionless*
QOQI	QO / average inflow rate	*dimensionless*
HI	The average stage (averaged over the duration of the inflow hydrograph)	*ft*
HR	The stage of the riser	*ft*
HIHR	(HI - HR)/HI	*dimensionless*

Table 14.6.2. c_t and c_d models for small impoundments.

Particle Size Class	Estimation Model	r^2	Mean	RMSE	Correlation
Clay	$c_t = 0.040 + 0.011(QOAIVS)$	0.37	0.115	0.177	NA
Silt	$c_t = 0.014 + 0.110(QOQI)^2$	0.77	0.042	0.016	NA
Sm. Agg.	$c_t = 0.015 + 0.127(QOQI)^2$	0.80	0.047	0.017	NA
Sand	$c_t = 0.006 + 0.255(QOAIVS)$	0.45	0.009	0.006	NA
Lg. Agg.	$c_t = 0.006 + 12.59(QOAIVS)$	0.77	0.011	0.006	NA
Clay	$c_d = 4.07$	NA	4.07	NA	NA
Silt	$c_d = 0.755 + 1.305(VMXVI) + 0.132(VPI)$	0.39	1.72	0.76	0.05
Sm. Agg.	$c_d = 0.466 + 2.753(VMXVI) + 0.058(VMX)$	0.56	2.21	0.74	0.11
Sand	$c_d = 0.632(QOAIVS)$	NA	0.006	0.014	NA
Lg. Agg.	$c_d = 41.67(QOAIVS) + 0.005(HI)$	NA	0.020	0.028	NA

Table 14.6.3. c_t and c_d models for large impoundments.

Particle Size Class	Estimation Model	r^2	Mean	RMSE	Correlation
Clay	$c_t = 0.101 + 0.049(QOAIVS) + 0.118(HIHR)$	0.78	0.071	0.019	0.21
Silt	$c_t = 0.002 + 0.125(QOQI)$	0.76	0.071	0.020	NA
Sm. Agg.	$c_t = 0.040 + 0.193(QOQI) + 0.041(VMXVI)$	0.76	0.098	0.033	0.12
Sand	$c_t = 0.004 + 3.105(QOAIVSE) \cdot 0.005(HIHR)$	0.95	0.018	0.002	0.19
Lg. Agg.	$c_t = 0.008 + 12.44(QOAIVSE) \cdot 0.012(HIHR)$	0.92	0.029	0.005	0.19
Clay	$c_d = 1.0$	NA	2.11	NA	NA
Silt	$c_d = 0.002(VMX) + 3.831(HIHR)$	NA	1.74	0.85	0.71
Sm. Agg.	$c_d = 0.004(VMX) + 3.124(HIHR)$	NA	1.68	0.13	0.71
Sand	$c_d = 0.075 + 17.71(QOARVS) \cdot 0.0002(VI)$	0.38	0.06	0.14	0.37
Lg. Agg.	$c_d = 0.576 + 172.4(QOARVS) + 0.359(VMXVI)$	0.53	0.33	0.35	0.57

14.6.3 Quiescent Settling During No Flow Conditions

After the water surface stage falls below the inlet stage of the lowest outlet structure, the only outflows are due to evaporation and infiltration and the impoundment experiences quiescent settling. To determine settling for each day during periods of no flow, quiescent settling theory is utilized. First, the depth of the interface between clear water and sediment-laden water is determined for each particle size subclass with the settling velocity for the subclass as follows:

$$H_{set} = H - V_s\ T \qquad [14.6.12]$$

where H_{set} is the depth of the interface (ft), V_s is the settling velocity ($ft \cdot s^{-1}$), and T is the duration of no flow conditions (time period with no flow). When the depth of the interface is known, the area, A_{set}, of the impoundment at the interface depth (ft^2) and volume, $\forall_{set}$ (ft^3), of the impoundment below the interface depth are computed. The concentration of sediment in the sediment-laden portion of the impoundment volume, C_{set} ($lbs \cdot ft^{-3}$), is determined using the ratio of impoundment volume, Vol (ft^3), to the sediment-laden volume of the impoundment, $\forall_{set}$, and the overall concentration of sediment in the impoundment, C_o ($lbs \cdot s^{-1}$), or:

$$C_{set} = C_o \left(\frac{\forall}{\forall_{set}} \right) \qquad [14.6.13]$$

The total deposition for the particle size subclass is computed using the concentration of sediment in the sediment-laden portion of the impoundment, C_{set}, the area at the sediment-laden interface, A_{set}, the settling velocity, V_s, and the duration of a day, T, by:

$$DEP = MIN \left((C_{set}\ V_s\ A_{set}\ T)\ ,\ (C_{set}\ \forall_{set}) \right) \qquad [14.6.14]$$

The total deposition in any one day cannot be greater than the total amount of sediment in the impoundment, hence the use of the minimum function in Eq. [14.6.14]. The new particle size subclass concentration, C_{on} ($lbs \cdot ft^{-3}$), is computed from the concentration at the beginning of the day, C_o, and the impoundment volume, ~~V~~, or

$$C_{on} = \frac{C_o \text{~~}V\text{~~} - DEP}{\text{~~}V\text{~~}} \qquad [14.6.15]$$

14.7 Validation

Detailed validation information is presented in other publications. However, the performance of WEPPSIE can be summarized as follows:

1. **Hydraulic Routing.** The hydraulic routing procedure is very comparable to the PULS routing procedure included in the CSTRS model. Further, the WEPPSIE routing procedure utilizes continuous outflow functions which eliminate errors due to linear interpolation between discrete stage-discharge points. Plus, the WEPPSIE routing procedure includes an adaptive step size which enables it to perform faster than the procedure in the CSTRS model.

2. **Stage-Discharge Relationships.** The outflow functions utilized for drop spillways and culverts have been well validated in the literature. The regression relationships utilized for perforated risers and open channels provide reasonable approximations of the stage-discharge relationships computed with more complex, iterative procedures that have been validated. The outflow function for rock-fill check dams should perform well given the limiting assumptions upon which it is based upon. The outflow function for filter fence and straw bales based on slurry flow rates has been widely used. However, slurry flow rates are highly dependent on the sediment content of the water and current values do not take into account clogging. These effects should be considered by the user.

3. **Sedimentation Algorithms.** The sedimentation algorithms including the calibration coefficient estimation models presented in Tables 14.3.2 and 14.3.3 have been validated against both a large data set created with the CSTRS model, and empirical data collected on a pilot scale impoundment. As compared to the CSTRS data set, WEPPSIE predicted trapping efficiencies within 2.6 % of those predicted by the CSTRS model on average. WEPP users should note that, for clay particles, WEPPSIE predicted trapping efficiencies consistently higher than the CSTRS model (four percent on average). As compared to the empirical data set, WEPPSIE predicted trapping efficiencies within 5.5 % of the observed trapping efficiencies and the WEPPSIE trapping efficiency predictions were consistently lower than the observed trapping efficiencies.

14.8 References

Barfield, B.J., R.C. Warner, and C.T. Haan. 1981. Applied Hydrology and Sedimentology for Disturbed areas. Oklahoma Technical Press, Stillwater, OK.

Chow, V.T. 1959. Open Channel Hydraulics. McGraw-Hill, New York, NY.

Federal Highway Administration. 1985. Hydraulic Design of Highway Culverts. Hydraulic Design Series No 5. Report No. FHA-IP-85-15, FHA, Washington, D.C.

Fogle, A.W. and B.J. Barfield. 1992. Channel-A Model of Channel Erosion by Shear, Scour, and Channel Headwall Propagation: Part 1 Model Development. Research Report No. 186, University of Kentucky, Water Resources Research Institute, Lexington, KY.

Foster, G.R. and L.J. Lane. 1987. User Requirements: USDA - Water Erosion Prediction Project (WEPP). NSERL Report # 1, USDA-ARS National Soil Erosion Research Laboratory, West Lafayette, IN.

Foster, G.R., R.A. Young, and W.H. Neibling. 1985. Sediment composition for nonpoint source pollution analyses. Transactions of the ASAE 28(1):133-139,146.

Griffin, M.L., B.J. Barfield, and R.C. Warner. 1985. Laboratory studies of dead storage in sediment ponds. Transactions of the ASAE 28(3):799-804.

Griffin, M.L. 1983. Characterizing the Hydraulic Efficiency of Sediment Ponds. M.S. Thesis. University of Kentucky, Lexington, KY.

Haan, C.T., B.J. Barfield, and J.C. Hayes. 1994. Design Hydrology and Sedimentology for Small Catchments. Academic Press, New York.

Haan, C.T. and H.P. Johnson. 1967. Geometrical properties of depressions in north-central Iowa. Iowa State Journal of Science 42(2):149-160.

Kohler, M.A., T.J. Nordenson, and W.E. Fox. 1955. Evaporation from Pans and Lakes. U.S. Weather Bureau Research Paper No. 38.

Laflen, J.M. 1972. Simulation of Sedimentation in Tile-Outlet Terraces. Ph.D Dissertation. Iowa State University, Ames, IA.

Lindley, M.R., B.J. Barfield, B.N. Wilson, and J.M. Laflen. 1993. WEPP surface impoundment element: farm pond sedimentation. ASAE Paper No. 932108. Presented at ASAE Meeting, Spokane, WA. American Society of Agricultural Engineers, St. Joseph, MI.

McEnroe, B.M., J.M. Steichen, and R.M. Schweiger. 1988. Hydraulics of perforated riser inlets for underground-outlet terraces. Transactions of the ASAE 31(4):1082-1085.

Press, W.H., S.A. Teukolsky, W.T. Vetterling, and B.P. Flannery. 1986. Numerical Recipes in FORTRAN: The Art of Scientific Computing. Cambridge University Press, Cambridge, New York.

Rochester, E.W. and C.D. Busch. 1974. Hydraulic design for impoundment terraces. Transactions of the ASAE 17(4): 694-696.

Schwab, G.O., R.K. Frevert, T.W. Edminster, and K.K. Barnes. 1981. Soil and Water Conservation Engineering. 3rd Edition. John Wiley and Sons, New York, NY.

Soil Conservation Service. 1984. Engineering Field Manual. USDA, Washington, D.C.

United States Department of Agriculture. 1980. CREAMS - A Field Scale Model for Chemicals, Runoff, and Erosion from Agricultural Management Systems. USDA Conservation Research Report No. 26, Washington D.C.

Ward, A.D., C.T. Haan, and B.J. Barfield. 1979. Prediction of sediment basin performance. Transactions of the ASAE 22(1):126-136. Water Resources Research 21(4):423-432.

Wilson, B.N. and B.J. Barfield. 1984. A sediment detention pond model using CSTRS mixing theory. Transactions of the ASAE 27(5):1339-1344.

Wilson, B.N. and B.J. Barfield. 1985. Modeling sediment detention ponds using reactor theory and advection-diffusion concepts. Water Resources Research 21(4):423-432.

14.9 List of Symbols

Symbol	Definition	Units
ΔH_1	change in head calculated at t, H	ft
ΔH_2	change in head calculated at $t + \Delta t/2,\ H + \Delta H_1/2$	ft
ΔH_3	change in head calculated at $t + \Delta t/2,\ H + \Delta H_2/2$	ft
ΔH_4	change in head calculated at $t + \Delta t,\ H + \Delta H_3$	ft
Δt	length of the computational time step	s
Δt_{next}	new computational time step based on $E_{\max}$	s
a	coefficient for equation 14.3.11	-
a_L	power function coefficient for flow length in equation 14.6.9	-
A	coefficient for regression equation relating discharge to head	$ft^3 \cdot s^{-1}$
A_{imp}	water surface area in impoundment	ft^2
$\bar{A}$	average impoundment surface area	ft^2
A_{cs}	cross sectional area of culvert	ft^2
A_o	cross sectional area of orifice	ft^2
A_p	cross-sectional flow area	ft^2
A_{PR}	regression coefficients for perforated riser, equation 14.3.5	$ft^{-3} \cdot s$
A_{set}	area of sediment clear-water interface	ft^2
b	coefficient for equation 14.3.11	-
B	coefficient for regression equation relating discharge to head	$ft^2 \cdot s^{-1}$
b_L	power function coefficients for flow length in equation 14.6.9	
B_{PR}	regression coefficients for perforated riser, equation 14.3.5	$ft^{-2.5} \cdot s$
c	culvert constant, given in Table 14.3.1	-
C	coefficient for regression equation relating discharge to head	$ft \cdot s^{-1}$
C'	dimensionless orifice coefficient (1)	-
C_{weir}	weir coefficient	$ft^{0.5} \cdot s^{-1}$
c_d	dimensionless parameter in equation 14.6.11	-
C_i	inflow sediment concentration	$lbs \cdot ft^{-3}$
c_L	power function coefficients for flow length in equation 14.6.9	-
C_o	outflow sediment concentration	$ft^3 \cdot s^{-1}$
C_{on}	outflow sediment concentration at end of computational time step	$lbs \cdot ft^{-3}$
C_{set}	concentration of sediment in sediment-laden volume during quiescent settling	$lbs \cdot ft^{-3}$
c_t	dimensionless parameter in equation 14.6.11	-
C_t	dimensionless empirical parameter for detention time in equation 14.6.7	-
D	coefficient for regression equation relating discharge to head	s^{-1}
$D_{culvert}$	interior height of culvert	ft
Dep	cumulative deposition in impoundment	lbs
dH/dl	dimensionless head loss gradient in rock-fill check dam	$ft \cdot ft^{-1}$
dia_{RF}	average rock diameter	m
dM/dt	time rate of change in total mass in the impoundment	$lbs \cdot s^{-1}$
DS	fraction of impoundment that is dead storage	$ft^3 \cdot ft^{-3}$
E	coefficient for regression equation relating discharge to head	$ft^{-1} \cdot s^{-1}$
$E_{\max}$	maximum numerical error for changing time step in equation 14.2.8 &9	ft
$E_{\min}$	minimum numerical error for changing time step in equation 14.2.7	ft

E_{vap}	actual evaporation from impoundment	$mm \cdot d^{-1}$
$f_A(H)$	function relating area to head	ft^2
$f_{Qo}(H)$	function relating discharge to head	$ft^3 \cdot s^{-1}$
g	gravitational constant	$ft \cdot s^{-2}$
H	average settling depth in reservoir	ft
H	water surface stage, head on flow control device	ft
H'	driving head for pipe flow	ft
H_{ff}	inlet stage for filter fence (stage at which flow begins)	ft
H_{new}	head (stage) at end of computational time step	ft
H_{ot}	stage at which flow control device overtops	ft
H_{sb}	inlet stage for straw bales (stage at which flow begins)	ft
H_{set}	depth of the interface between sediment laden water and clear water for a given particle size	ft
HW_i	headwater depth for culvert flow	ft
$Infil$	daily head loss from impoundment due to infiltration	$ft \cdot d^{-1}$
K	culvert constant, given in Table 14.3.1	-
K_b	dimensionless bend head-loss coefficient	-
K_c	friction loss coefficient	ft^{-1}
K_e	dimensionless entrance head-loss coefficient	-
K_{sat}	saturated hydraulic conductivity of the layer controlling infiltration	$ft \cdot h^{-1}$
L	length of the weir	ft
L	flow length through impoundment	ft
L	flow length of pipe	ft
L_{RF}	flow length through the rock-fill	m
M	mass of sediment in impoundment	lbs
M	culvert constant, given in Table 14.3.1	-
PET	potential evaporation from impoundment	$mm \cdot d^{-1}$
$Q_{culvert}$	discharge from a culvert	$ft^3 \cdot s^{-1}$
$Q_{drop\ spillway}$	flow in drop spillway	$ft^3 \cdot s^{-1}$
$Q_{filter\ fence\ or\ straw\ bale}$	discharge rate controlled by slurry flow rate	$ft^2 \cdot s^{-1}$
Q_i	inflow rate into impoundment	$ft^3 \cdot s^{-1}$
Q_o	outflow rate from impoundment	$ft^3 \cdot s^{-1}$
$Q_{orifice}$	discharge through an orifice	$ft^3 \cdot s^{-1}$
$Q_{perforated\ riser}$	discharge from spillway with a perforated riser	$ft^3 \cdot s^{-1}$
Q_{pipe}	discharge from control device when flowing as pipe flow	$ft^3 \cdot s^{-1}$
$Q_{rock-fill}$	flow rate through rock-fill check dam	$m^3 \cdot s^{-1}$
Q_{slots}	discharge from preforated riser when controlled by slots	$ft^3 \cdot s^{-1}$
$Q_{submerged}$	discharge in a culvert when inlet is submerged	$ft^3 \cdot s^{-1}$
$Q_{unsubmerged}$	discharge through a culvert when inlet is unsubmerged, equation 14.3.7	$ft^3 \cdot s^{-1}$
Q_{weir}	discharge over a wier	$ft^3 \cdot s^{-1}$
S	culvert barrel slope	$ft \cdot ft^{-1}$
t	time	s
T	duration of zero flow	s
T_{day}	time step of 24 hours	h
t_D	detention time	s
$t_{D\,100}$	detention time required for 100% of a given particle size to settle out of suspension	s

$\overline{V}$	impoundment volume at beginning of time step	ft^3
V_c	overflow rate	$ft \cdot s^{-1}$
$\overline{V}_n$	impoundment volume at end of the time step	ft^3
Vol	average impoundment volume over computational time step	ft^3
V_s	particle settling velocity	$ft \cdot s^{-1}$
V_{set}	sediment-laden volume during quiescent settling	ft^3
V_{sl}	slurry-flow rate for filter fence or straw bales	$ft \cdot s^{-1}$
W_b	bottom width of filter fence or straw bale check dam	ft
wd_{ff}	width of the filter fence	ft
wd_{rf}	width of the rock-fill check dam	m
wd_{sb}	width of the straw bales	ft
Y	culvert constant, given in Table 14.3.1	-